

Controlling the yield behavior of fat-oil mixtures using cooling rate

Sashikumar Ramamirtham¹ · A. Shahin² · Madivala G. Basavaraj¹ · Abhijit P. Deshpande¹

Received: 31 March 2017 / Revised: 31 August 2017 / Accepted: 13 September 2017 / Published online: 3 October 2017
© Springer-Verlag GmbH Germany 2017

Abstract The rheological behavior such as yielding of fat crystal networks are dictated by many variables. Among these variables, the shape of the constituent fat cluster is important yet relatively unexplored. In this work, we describe the rheological investigations of a fat-oil system which can be formulated to either contain bundles of needles or spherical clusters by controlling the cooling rate and fat concentration. Fat-oil mixtures containing high-fat concentrations exhibited weak frequency dependence of storage modulus (G') and loss modulus (G''). The yielding behavior of the mixtures were investigated by large amplitude oscillatory shear (LAOS) rheology using strain and stress controlled modes. Lissajous-Bowditch plots and orthogonal set of Chebyshev polynomials were used to analyze the non-linearities associated with the yielded fat-oil mixtures. For a given fat concentration, the yield stress of fat networks obtained at low cooling rates (bundles of needles) were similar to that of networks obtained at high cooling rates (spherical clusters). However, after yielding, Lissajous-Bowditch plots suggested that the mixtures comprising of bundles of needles exhibited viscous-like behavior while the spherical clusters exhibited a plastic-like behavior. This was further

supported by microscopy images of yielded fat-oil mixtures. Overall, for a given fat concentration, the two different shapes of fat clusters can give rise to networks of similar yield stress values but different behaviors after yielding.

Keywords Fat-oil mixtures · Fat crystal networks · Microstructure · Cooling rate · Yield stress · Large oscillatory shear rheology (LAOS) · Non-linear rheology

Introduction

Many products in food and cosmetic industries such as shortenings, mayonnaise, chocolates, and cold creams are formulated to achieve desired properties to satisfy specific consumer requirements (De Graef et al. 2011; Ma and Barbosa-Cánovas 1995). Fats find application in cosmetic products typically as oil phase thickeners. Few examples of such materials include candelilla wax, bees wax, and syn-crowax (Toro-Vazquez et al. 2007). The macroscopic physical properties such as the texture and sensorial attributes of the fat-oil mixtures are related to their rheological behavior such as yielding and thixotropy (Suzuki and Watanabe 1971; Macias-Rodriguez and Marangoni 2016). The rheological behavior of the fat-oil mixtures are in turn dictated by the morphology of the constituent fat crystal network that can be engineered by controlling the processing conditions, in particular fat concentration and cooling rate (Narine and Marangoni 1999b; Herrera and Hartel 2000a; Ramamirtham et al. 2017). The processing conditions affect the kinetics of crystallization as well as cluster formation thereby giving rise to different crystal morphologies. Hence, understanding the yielding behavior of different fat crystal morphologies provides the necessary knowledge to formulate products with specific properties (Narine and Marangoni 2002).

Electronic supplementary material The online version of this article (<https://doi.org/10.1007/s00397-017-1048-6>) contains supplementary material, which is available to authorized users.

✉ Madivala G. Basavaraj
basa@iitm.ac.in
Abhijit P. Deshpande
abhijit@iitm.ac.in

¹ Department of Chemical Engineering, Indian Institute of Technology Madras, Chennai, 600036, India

² Unilever R & D Bangalore, Bangalore, India

Fat crystal network comprises structures of varying length scales, namely, the triglyceride (TAG) chains, crystal lamellae, single crystal, and crystal clusters (Marangoni et al. 2012; Acevedo and Marangoni 2010). TAG chains can also self-assemble in different ways leading to different polymorphs. Overall, the cooling rate can be used to control the cluster formation thereby tuning the size and shape of fat clusters. Moreover, the rheological responses of fat crystal networks can be different due to the differences in their underlying microstructures. Additionally, the morphology of the fat crystal networks used in food industries has been shown to evolve with time. Hence, the age of the sample is also expected to play a major role in the rheological response (Chen and Terentjev 2009).

The rheological responses have been used to characterize the morphology of fat crystal networks using fractal analysis (Vreeker et al. 1993; Narine and Marangoni 1999a; Tang and Marangoni 2006; Gao et al. 2006; da Silva and Coutinho 2004). At high-fat concentrations, the elastic strength of inter-clustural links in the fat network prevail over the elastic strength of individual clusters, and thus, the fat network is believed to be in a weak-link regime (Shih et al. 1990). It has been shown that the important rheological parameters such as storage modulus (G') and yield stress scales with the fat concentration (ϕ) in a power law manner (Vreeker et al. 1993; Marangoni and Rogers 2003). Further, Herrera and Hartel studied the effect of cooling rate on crystal size distribution and their rheological properties (Herrera and Hartel 2000a). They showed that G' values were higher for milk fat containing bigger crystals (Herrera and Hartel 2000b).

The technique of large amplitude oscillatory shear (LAOS) has been used to understand the yielding and non-linearities of colloidal and polymer systems (Renou et al. 2010; Khandavalli and Rothstein 2015). Renou et al. (2010) suggested yielding mechanisms for colloidal glass comprised of star-like polymer micelles using LAOS. Recently, Macias-Rodriguez and Marangoni (2016) showed the importance of understanding the non-linearities of fat systems using LAOS. This study characterized the yielding behavior of various commercial triglyceride shortenings of different compositions. The authors remarked that despite different compositions of the triglycerides, they exhibited comparable G' in linear viscoelastic region (LVR) and yield stresses. However, they also showed that these triglycerides exhibit prominent differences in their non-linear viscoelastic behavior through elastic Lissajous-Bowditch plots after yielding. Since different triglycerides have different morphologies, deriving the structure-rheology relationship becomes difficult and complex. Hence, for better understanding of the structure-rheology relationship, a fat-oil system of tunable microstructure which leads to different rheological behavior is desirable.

In this work, syncrowax-HRC, a TAG that is used as a thickening agent in personal care products, was used along with isopropyl myristate (oil) as a model system to understand the effect of cluster shape on the thixotropic nature and yielding behavior of fat-oil mixtures. It has been shown in our previous study that the fat clusters of different shapes such as spherical and bundles of needles can be engineered by precise control of cooling rate (Ramamirtham et al. 2017). At sufficiently high-fat concentration, these clusters held together by van der Waals forces give rise to a space spanning interconnected 3D network which entraps the oil phase. A schematic representation of the space spanning networks comprising spherical fat clusters and bundles of needles is shown in Fig. 1 (Ramamirtham et al. 2017). Firstly, the thixotropic nature of the fat-oil mixtures was studied using shear rate sweeps. Subsequently, the linear and non-linear viscoelastic rheological responses of the fat-oil mixtures were captured using LAOS experiments performed by stress- and strain-controlled modes. We present the effect of cluster shape on the rheological response before and after yielding using Lissajous-Bowditch plots and intra-cycle non-linearities along with microscopy images.

Materials and methods

Materials

Tribehenin (2,3-di(docosanoyloxy)propyl docosanoate) with a molecular formula of $C_{69}H_{134}O_6$ is a triglyceride of glycerin and behenic acid, a naturally occurring long-chain fatty acid. It is commonly used as an oil phase thickener. Tribehenin commercially available as syncrowax-HRC was obtained from Croda Chemicals (India). The purity of tribehenin in syncrowax-HRC as provided by the supplier is around ≥ 90 wt%. The melting point of syncrowax-HRC measured from various DSC measurements is 332.6 K. The oil phase isopropyl myristate (IPM) is an ester of isopropanol and myristic acid. IPM ($C_{17}H_{34}O_2$) was

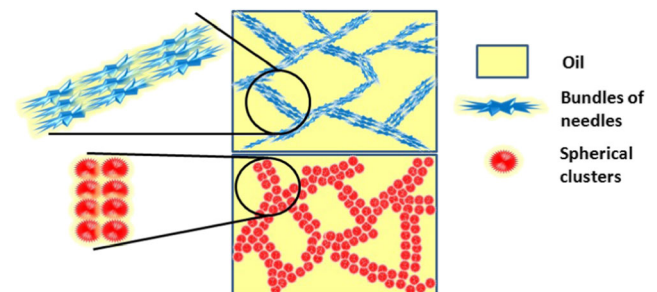


Fig. 1 Schematic representation (2D) of fat crystal networks constituted by two different shapes of clusters

purchased from Sigma-Aldrich (98% purity, CAS Number 110-27-0). The melting and boiling points of IPM are 276 and 588 K (at 760 mmHg) respectively (provided by the supplier). The density of IPM at 298 K is 850 kg/m^3 and density of tribehenin is 890 kg/m^3 .

Sample preparation

The fat-oil mixtures were prepared in clean, dry glass vials. The total weight of each mixture was maintained at 10 g. The mixtures were prepared at fat concentrations of 7.5, 10, 15, 20, and 25 wt%. The fat concentrations were converted to volume% for fractal dimension calculations. These mixtures were placed in an environmental chamber (Memmert CTC256, Germany) maintained at 353 K for 1 h to completely dissolve the fat in oil. After this, homogeneous and transparent solutions of fat-oil mixtures were obtained. These mixtures were then cooled to 293 K at cooling rates of 0.1, 0.5, 1, and 2.0 K/min. The chamber is equipped with platinum temperature sensors along with microprocessor temperature controller. The temperature controller has an integrated timer which can be used to ramp temperatures linearly in a given time thereby controlling the cooling rate. Hence, for crystallizing the samples at 0.1 K/min, the temperature was ramped down from 353 to 293 K in 600 min. Similarly, the ramping down time was controlled to prepare samples at different cooling rates. After cooling, the samples were held at 293 K for 24 h. Since the chamber could not be used to attain cooling rates higher than 2 K/min, higher cooling rates were attained by cooling the fat-oil mixtures in a constant temperature water bath. For the preparation of fat-oil mixtures at high cooling rates, water bath maintained at 278 K was used. The cooling time for these samples was 2 h. The cooling profile of these mixtures was measured and the average cooling rate was calculated to be 9 K/min (see [Supplementary Information](#)). All the samples were prepared in duplicate to ensure consistency. All the samples were characterized after an equilibration time of 24 h. The samples were stored at 298 K. XRD and DSC of 24 h and 3-month old samples (see [Supplementary Information](#)) were used to verify that the samples reached their equilibrium structure and there was no effect of aging.

Microscopy

The microstructures of the fat crystals were recorded using an inverted optical microscope DMI3000 B from Leica, Germany. Bright-field mode was used with objectives of magnifications $10\times$ and $63\times$. Approximately $10 \mu\text{l}$ of fat-oil mixture was placed on a glass slide at room temperature and the crystals were viewed at different magnifications.

Since the samples were opaque at high-fat concentrations, imaging was done by diluting the sample to approximately 5 wt% fat. The dilution was done only to improve the quality of optical microscopy images and did not affect the size and morphology of the individual fat crystal clusters.

Rheology

A parallel plate geometry (rough) of diameter 25 mm was used at a gap of 0.8 mm. The roughness of the geometry was $46.2 \mu\text{m}$. The shear rate sweeps were carried out in MCR 301 (Anton Paar, Austria). The small amplitude oscillatory shear (SAOS) rheology and LAOS rheology experiments were performed on MCR 301 and MCR 702 (Anton Paar, Austria). The measurements were carried out on MCR 702 using a twin drive (single rotation and single transducer mode). The roughened geometry was used to apply oscillatory strain while a smooth parallel plate geometry of 25-mm diameter was used as the transducer. All the experiments were carried out at 298 K. Experiments at different gaps using both smooth and rough geometry were used to rule out any effect of wall slip as shown in Fig. 2. All the measurements were done in triplicate.

Shear rate sweeps

Shear rate sweeps were performed to measure viscosity by increasing the shear rate in a logarithmic manner from 0.001 to 500 s^{-1} and subsequently decreasing it from 500 to 0.001 s^{-1} . The measurement time for each data point was fixed at 20 s.

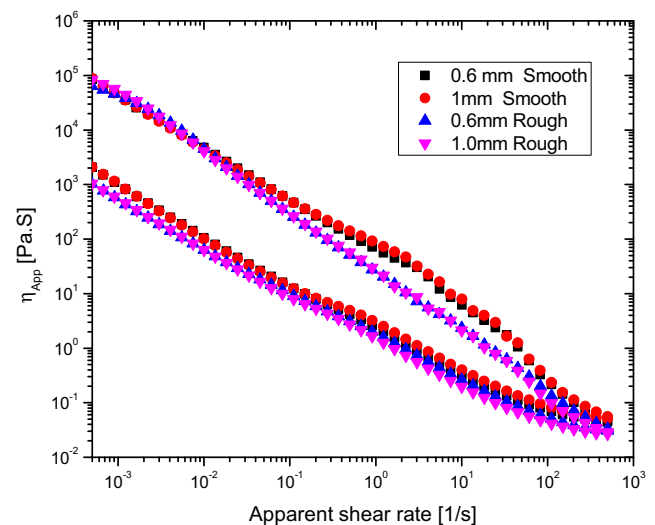


Fig. 2 Forward and reverse shear rate sweeps performed at different gaps for 15 wt% fat-oil mixtures cooled at 0.5 K/min using smooth and rough geometry

SAOS

Oscillatory stress sweeps (MCR 301) and strain sweeps (MCR 702) were carried out at a fixed frequency. Frequency sweeps were performed at 0.01% strain amplitude. The G' and G'' are independent of frequency in the frequency range of 1 to 100 rad/s. The strain and stress sweeps were performed at constant frequency of 1, 5, and 10 rad/s. The fat-oil mixtures were subjected to increasing oscillatory shear stress from 0.01 to 1000 Pa in logarithmic manner while the strain amplitude sweep was performed from 0.001 to 1000%. The measurement time for each data point was fixed at 20 s. Henceforth, stress amplitude sweeps carried out using MCR 301 are referred to as “stress-controlled” experiments. Similarly, strain amplitude sweeps carried out using MCR 702 are referred to as “strain-controlled” experiments.

LAOS

Dynamic strain sweeps from strain amplitude of 0.001 to 1000% in a logarithmic manner were carried out at a fixed frequency. The measurement time for each data point was fixed at 20 s. Furthermore, the Lissajous-Bowditch plots were obtained along with various non-linear measures from the Physica software RheoCompass. These values were verified by analyzing each oscillation data using MITlaos software (Ewoldt et al. 2007). The qualitative nature of the Lissajous-Bowditch plots were verified at different shear histories by performing strain sweeps at different measurement points/decades (data not shown). All the non-linear

viscoelastic measures had a standard deviation of around 5–10% from three replicated measurements.

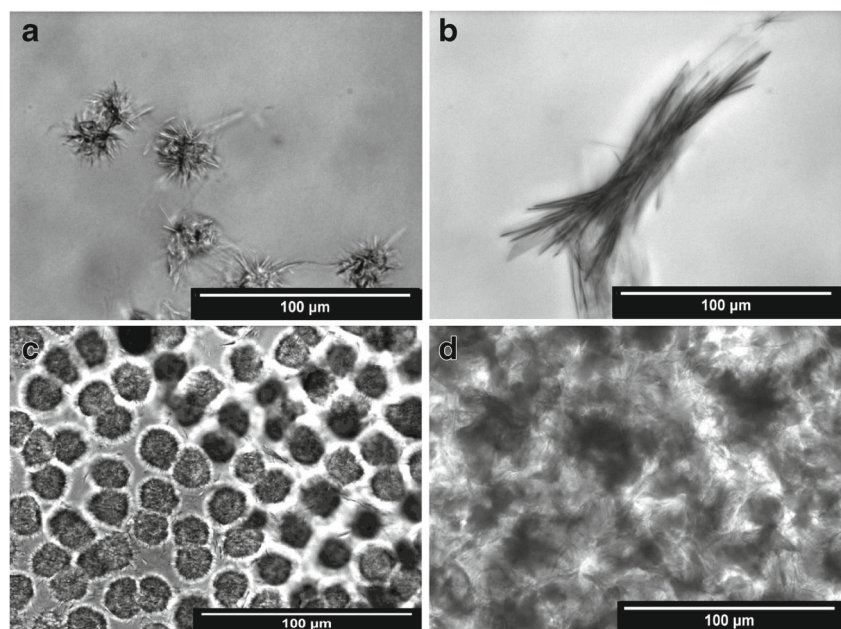
Statistics

For a given fat concentration, regression analysis was performed to find the correlation between cooling rate and yield stress values using a level of significance of 0.05. Statistical analysis was performed by Microsoft Excel 2007 data analysis tool pack. Curve fittings were done using Origin 8.5 software. A linear fit $y = a + bx$ was used to derive the fractal dimension from the yield stress vs fat concentration data. For all the fits, Pearson's r values are in the range of 0.95–0.99.

Results

A detailed phase behavior of tribehenin in IPM has been reported in our earlier work (Ramamirtham et al. 2017). In here, we consider tribehenin-IPM gels at sufficiently high-fat concentrations (>7 wt%). In particular, the fat crystal networks comprising clusters of two distinct shapes, namely, bundles of needles and spherical clusters as shown in Fig. 3, were investigated. The rheological investigations were conducted for the mixtures in uniform gel phase which did not flow when the sample vial containing them was tilted. Unlike many fat-oil mixtures used in food industry, the fat-oil system used in this study does not exhibit considerable morphological evolution with aging and is stable for up to 3 months (see [Supplementary Information](#)).

Fig. 3 Microscopy pictures of constituent clusters (**a**, **b**) and their respective fat crystal networks (**c**, **d**). **a** shows spherical clusters obtained after dilution of the network (**c**) formed by 15 wt% fat-oil mixture crystallized at 2 K/min. **b** shows bundles of needles obtained after dilution of the network (**d**) formed by 15 wt% fat-oil mixture crystallized at 0.1 K/min. Size of scale bar is 100 μm



Shear rate sweeps

Fat-oil mixtures at various concentrations prepared at different cooling rates were studied by measuring viscosity values through a shear rate sweep with 20 s measurement time for each data point. For a given fat concentration, the viscosity value for a mixture cooled at 0.1 K/min is highest followed by 9 K/min. The shear rate sweeps of 15 wt% fat-oil mixtures crystallized at different cooling rates are shown in Fig. 4. The viscosity values of all fat-oil mixtures decrease with increase in shear rate signifying their shear thinning behavior. Furthermore, it can be seen from Fig. 4 that all the fat-oil mixtures exhibit thixotropy and hysteresis as there is a difference in viscosity values obtained by forward (filled symbols) and reverse (open symbols) shear rate sweeps. Fat crystal networks comprising of bundles of needles crystallized at 0.1 and 0.5 K/min exhibit a drop in viscosity by 2–3 orders of magnitude during reverse shear rate sweep while the networks comprising of spherical clusters crystallized at 2 and 9 K/min exhibit a drop in viscosity by about an order of magnitude. This observation is consistent for all the fat concentrations that were studied (data not shown). The higher drop in magnitude of viscosity suggests a higher degree of breakdown of fat crystal network made of bundles of needles as compared to networks made of spherical clusters. Furthermore, the rebuilding time scale of all the fat-oil mixtures studied in this manuscript was much more than the measurement time scale. This was verified by performing successive forward and reverse shear rate sweeps as shown in Fig. 5. It can be seen from Fig. 5 that the viscosity values did not rebuild even after three shear rate cycles.

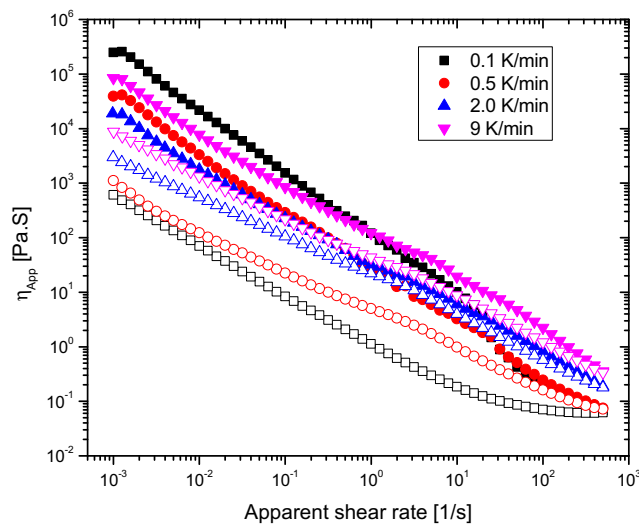


Fig. 4 Forward and reverse shear rate sweeps of 15 wt% fat-oil mixtures crystallized at different cooling rates. Filled symbols show the viscosity values obtained by increasing the shear rate from 0.001 to 500 s⁻¹ while open symbols show the viscosity values obtained by decreasing the shear rate from 500 to 0.001 s⁻¹

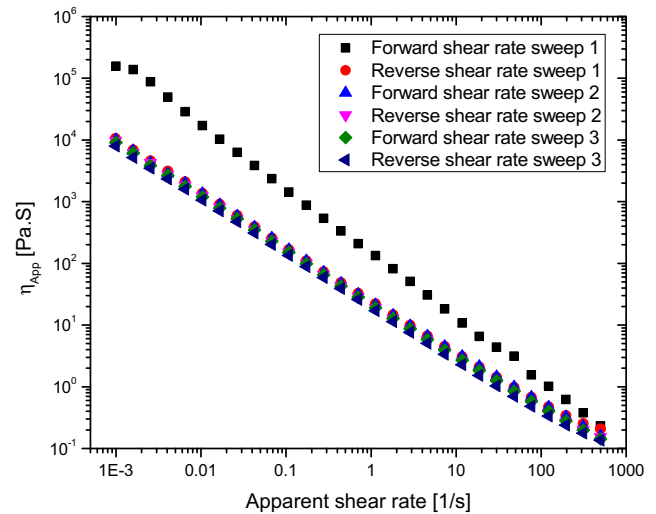


Fig. 5 Successive forward and reverse shear rate sweeps of 20 wt% fat-oil mixtures crystallized at 2.0 K/min

Hence, aging of the fat-oil mixtures did not play a significant role during the rheological measurements. The above result was further validated by performing successive forward and reverse strain sweeps in oscillatory mode (data not shown).

SAOS

For all the the fat-oil mixtures studied, G' is at least an order of magnitude higher than G'' and both remain almost independent of the frequency as shown in Fig. 6. For the frequency sweeps, a fixed strain of 0.01% was used which is well within the linear viscoelastic region (LVR) for all the fat-oil mixtures. The modulus values and yield strain

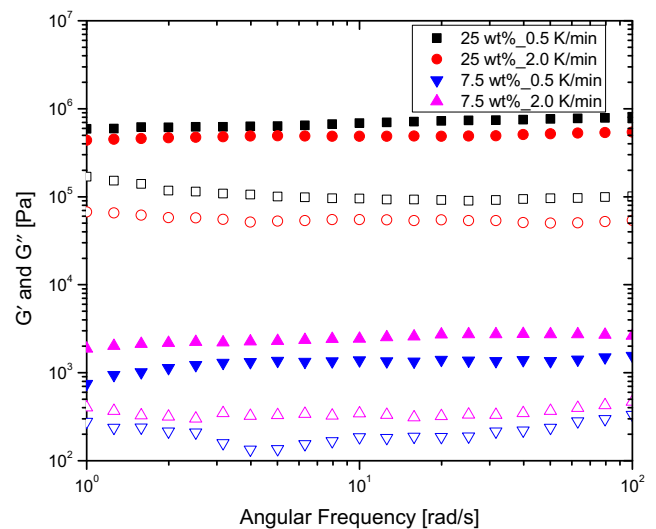


Fig. 6 Frequency sweeps showing G' (filled) and G'' (open) values for fat-oil mixtures having 25 wt% fat concentration cooled at 0.5 and 2.0 K/min along with 7.5 wt% fat concentration cooled at 0.5 and 2.0 K/min

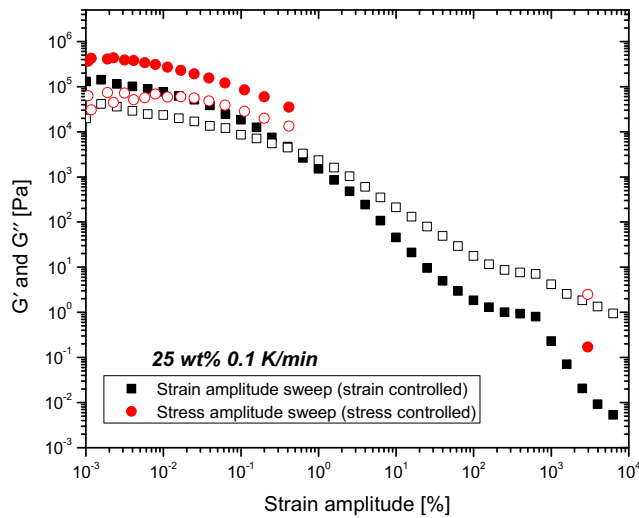


Fig. 7 Modulus values from strain-controlled and stress-controlled modes of 25 wt% fat-oil mixture cooled at 0.1 K/min at 10 rad/s

(crossover strain) for different cooling rates were obtained by both strain-controlled and stress-controlled modes. As an example, data obtained for 25 wt% fat-oil mixtures constituting different shaped fat clusters using both modes are shown in Figs. 7 and 8. The two modes of measurements carried out at 10 rad/s show similar qualitative features, though there are quantitative differences in modulus values. It is also worth noting that, in the stress-controlled measurements shown in Fig. 7, the network of bundles of needles (0.1 K/min) exhibits a steep decrease in modulus values and a steep increase in strain amplitude when the applied stress increased beyond the yield point (around 0.5% strain). This suggests a rapid breakdown of the structure beyond the yield point and correspondingly a jump in strain amplitude from 0.5 to about 1000% was observed. On the other hand, the

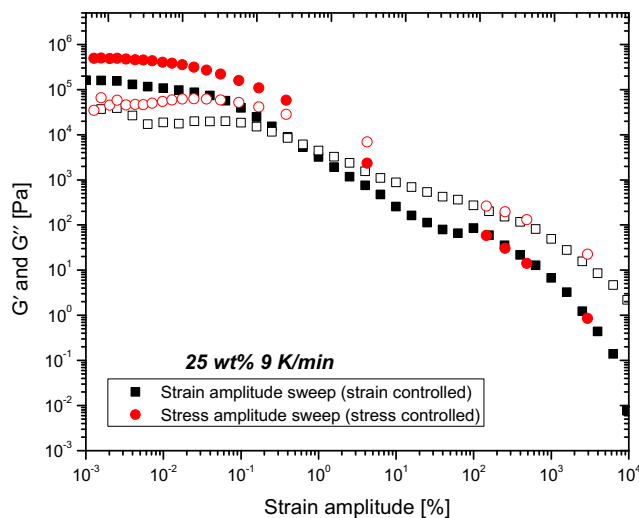


Fig. 8 Modulus values from strain-controlled and stress-controlled modes of 25 wt% fat-oil mixture cooled at 9 K/min at 10 rad/s

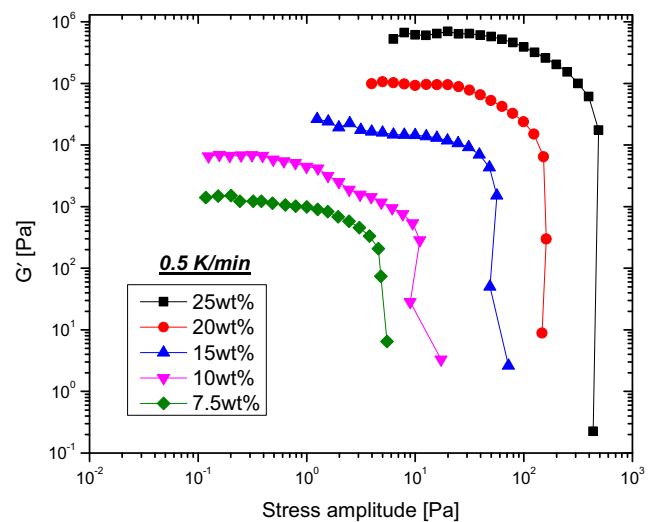


Fig. 9 Stress amplitude sweeps at 10 rad/s of fat-oil mixtures at various fat concentrations cooled at 0.5 K/min

network made of spherical clusters as shown in Fig. 8 shows a relatively gradual increase in strain after yielding, suggesting the breakdown of structure is not as rapid as the case of bundles of needles. Further, in the reverse strain amplitude sweep, the networks made of bundles of needles exhibit a bigger drop in modulus values as compared to the networks made of spherical clusters (data not shown). This behavior is in agreement with the shear rate sweep measurements.

G' values from oscillatory stress sweeps on different fat-oil mixtures performed at 10 rad/s using a stress-controlled mode are shown in the Figs. 9 and 10. The stress sweeps exhibit a LVR wherein the G' values nearly remain constant implying there is no breakdown of the structure. Beyond a critical value of stress, structural breakdown occurs causing

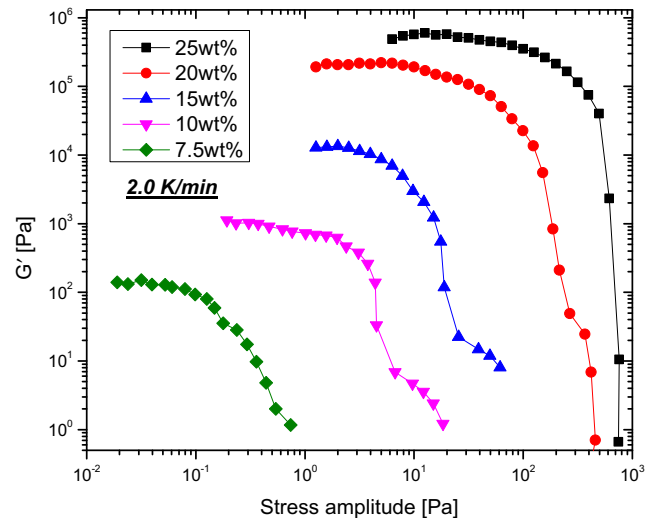


Fig. 10 Stress amplitude sweeps at 10 rad/s of fat-oil mixtures at various fat concentrations cooled at 2.0 K/min

Table 1 Yield stress (Pa) values at 10 rad/s for fat-oil mixtures at various initial fat concentrations and cooling rates

Cooling rate (K/min)	7.5 wt%	10 wt%	15 wt%	20 wt%	25 wt%
0.1	*	*	225 ± 25	627 ± 33	1125 ± 125
0.5	3 ± 2	10 ± 1	85 ± 25	127.5 ± 34.5	500 ± 10
1.0	1.5 ± 0.5	7 ± 2	39 ± 5	97 ± 13	300 ± 15
2.0	0.4 ± 0.5	2.2 ± 1.5	32.6 ± 12.4	173.3 ± 26.6	618 ± 5
9	*	32.5 ± 2.5	155 ± 10	405 ± 35	950 ± 50

* Yield stress values were not reported since samples were not uniform gels

the material to flow and this critical stress can be taken as the yield stress of the material. The breakdown of the structure is marked by a decrease in G' value. The stress value at which the G' and G'' cross over was taken as the yield stress of the material (Renou et al. 2010). The yield stress values of the fat-oil mixtures are shown in Table 1. There is no significant ($P > 0.05$) correlation between the cooling rate and yield stress values. For a given fat concentration, the yield stress values of networks made of bundles of needles at 0.1 and 0.5 K/min were comparable to that of networks made of spherical clusters at 9 and 2 K/min, respectively. The fractal dimensions of the networks were calculated from the yield stress values using the scaling theory for weak-link regime (Shih et al. 1990):

$$\sigma_0 \sim \phi^{[1/3-D]} \tag{1}$$

where σ_0 is the yield stress, ϕ is the particle concentration in the gel, and D is the fractal dimension. In the weak-link regime, the strength of links between fat clusters dominate over the strength of clusters themselves. This was further validated through microscopy images of fat-oil mixtures after yielding where the clusters remained intact (Ramamirtham et al. 2017). The power law relationship of

yield stress values with fat concentration was verified as shown in Fig. 11 and apparent fractal dimensions (D_{app}) are shown in Table 2. These fractal dimensions were in agreement with the ones derived from power law relationship of G' in our previous study (Ramamirtham et al. 2017).

After yielding, the networks made up of bundles of needles exhibit a steep decrease in G' values for a very small increase in stress as shown in Fig. 9 suggesting a rapid breakdown of the network. Similar behavior was observed at all fat concentrations for cooling rates 0.1 and 0.5 K/min (data not shown). For networks comprising of spherical clusters at 2 and 9 K/min, a more gradual yielding is observed as shown in Fig. 10. The above observations suggest that cluster morphology also dictates the breakdown mechanism of the fat crystal network upon yielding. To further probe this difference in behavior of fat networks after yielding, it is important to study their behavior at large strain amplitudes.

LAOS analysis

The G' and G'' values from the strain amplitude sweeps for 25 wt% fat-oil mixtures comprising of two different cluster shapes are shown in Fig. 12a. Corresponding torque amplitude values at different cooling rates are shown in the Fig. 12b. Similar to the observations from stress sweeps, the effect of cluster shape on the rheological behavior after yielding is clearly evident. In case of the networks comprising of bundles of needles obtained by cooling at 0.1 and 0.5 K/min, the torque begins to drop after yielding indicating breakdown of the structure. On the other hand, upon yielding of networks formed at 2 and 9 K/min, there is an

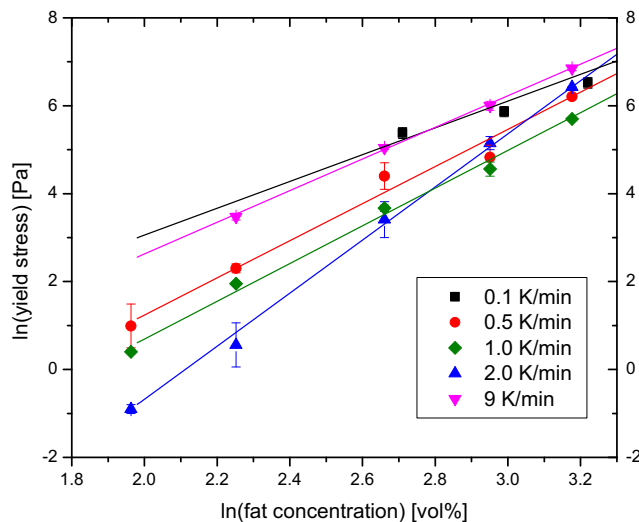


Fig. 11 Yield stress values (symbols) and power law fit (line) of fat-oil mixtures cooled at various cooling rates

Table 2 Apparent fractal dimensions (D_{app}) derived from yield stress values for various cooling rates

Cooling rate(K/min)	D_{app}
0.1	2.72
0.5	2.77
1.0	2.77
2.0	2.83
9	2.72

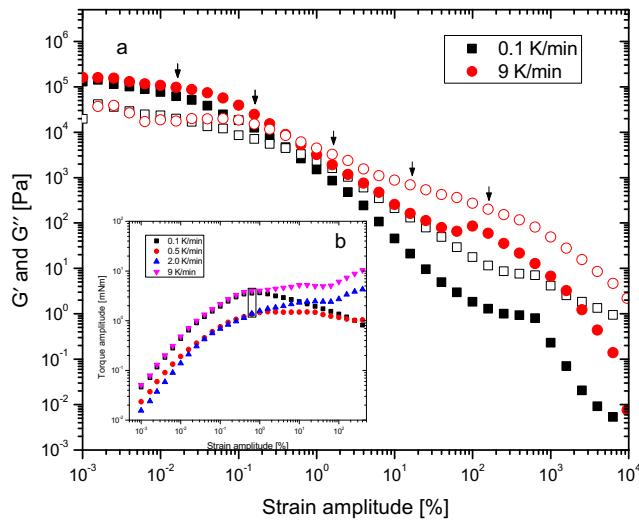


Fig. 12 **a** Modulus values from strain amplitude sweeps of 25 wt% fat-oil mixture cooled at 0.1 and 9 K/min at 10 rad/s. **b** Torque values obtained from dynamic strain sweeps at 10 rad/s for 25 wt% fat-oil mixtures cooled at various cooling rates. The boxed values indicate the point of yielding

increase in torque amplitude. This behavior is consistent for all fat concentrations for a given cooling rate (data not shown). The elastic Lissajous-Bowditch plots corresponding to the data points indicated with arrows in Fig. 12a are shown in Fig. 13. At low strain amplitudes of 0.01585% which is in the LVR region, both networks show viscoelastic signatures. At intermediate strain amplitudes of 1.585 and 15.85% (after yield), the Lissajous-Bowditch plots show almost a constant stress over a wide range of strain amplitudes suggesting a plastic-like response. Further, at a strain amplitude of 158.5%, the network comprising of bundles of needles exhibits viscous-like behavior while the network comprising of spherical needles remains plastic-like. Similar signatures were seen for fat crystal networks obtained at other cooling rates with similar cluster shapes (data not shown). This was also confirmed by microscopy images of the samples after yielding as shown in Fig. 14. Both the mixtures were paste-like materials before yielding while after yielding, the mixture with bundles of needles breaks down to a viscous dispersion. This dispersion contains individual fat clusters floating in a sea of oil (the brighter regions in Fig. 14a is oil). On the other hand, the mixture made up of spherical clusters remains in a paste-like form with the constituent clusters closely held together as shown in Fig. 14b. This is also evident in the Pipkin diagrams shown in the Fig. 15. Interestingly, at low frequencies of 1 and 5 rad/s, the Lissajous-Bowditch plots at high strain amplitudes of 15.85 and 158.5% for networks made of spherical clusters (Fig. 15b) show typical stress overshoots that are usually associated with cage breaking and reformation in polymer and colloidal systems (Renou et al. 2010). On the other

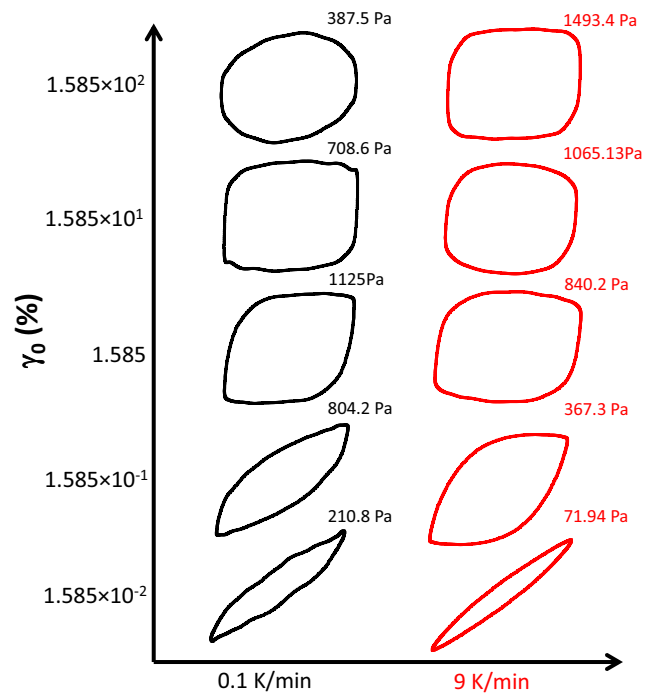


Fig. 13 Evolution of elastic Lissajous-Bowditch plots for different strain amplitude at a frequency of 10 rad/s for 25 wt% fat-oil mixtures comprising of different shaped fat clusters

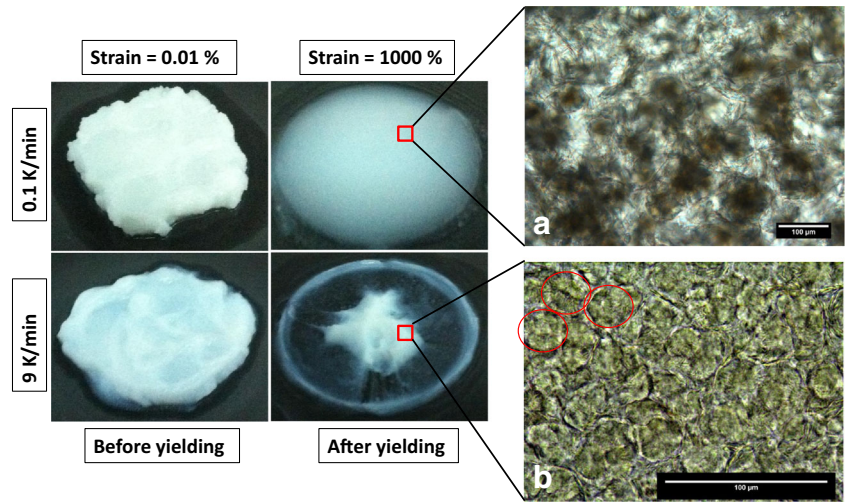
hand, the bundles of needles (Fig. 15a) show no such behavior. This suggests that the plastic-like response of networks comprising of spherical clusters at high strain amplitudes could be due to cluster rearrangements which is explained further in the discussion section.

Apart from the difference in the elastic Lissajous-Bowditch plots at very high strain amplitudes, fat networks made of different shaped fat clusters exhibit differences at strain amplitudes around the point of yielding (around 0.5%) as shown in Fig. 16. It can be observed from the elastic Lissajous-Bowditch plots that network made of bundles of needles (0.1 K/min) exhibits small yet distinct stress upturns at large strains as compared to network made of spherical clusters (2 K/min). This indicates a higher degree of strain hardening in case of bundles of needles, which gradually fades away after yielding at a strain amplitude of 1%. Although such stress overshoots and upturns have been shown in fat crystal networks (Macias-Rodriguez and Marangoni 2016), the above results suggest that such nonlinearities could be related to shape of the constituent fat clusters.

From the Lissajous-Bowditch curves, the dynamic modulus at minimum strain (G'_M) and dynamic modulus at large strain (G'_L) (Ewoldt et al. 2008) were obtained. From these variables, the stiffening ratio (S) was calculated.

$$G'_M = \left. \frac{d\sigma}{d\gamma} \right|_{\gamma=0}; G'_L = \left. \frac{\sigma}{\gamma} \right|_{\gamma=\pm\gamma_0}; S = \frac{G'_L - G'_M}{G'_L} \quad (2)$$

Fig. 14 Pictures of 25 wt% fat-oil mixtures comprising of different shaped fat clusters before and after yielding. **a** and **b** shows the bright-field microscopic images of these fat-oil mixtures after yielding



Similarly, the dynamic viscosity at minimum strain rate (η'_M) and dynamic viscosity at large strain rate (η'_L) were derived. The thickening ratio (T) was also calculated according to the following formula:

$$\eta'_M = \left. \frac{d\sigma}{d\dot{\gamma}} \right|_{\dot{\gamma}=0}; \eta'_L = \left. \frac{\sigma}{\dot{\gamma}} \right|_{\dot{\gamma}=\pm\dot{\gamma}_0}; T = \frac{\eta'_L - \eta'_M}{\eta'_L} \quad (3)$$

The abovementioned parameters help in understanding the behavior of the material in non-linear regime and in differentiating the yield behaviors of the networks comprising of two different shaped clusters. G'_M and G'_L for both types of clusters are shown in the Fig. 17 for a fat concentration of 25 wt%. For both mixtures, G'_M and G'_L were of similar values in the linear regime as well as during the initial stage of non-linear regime till the point of yielding ($\sim 0.5\%$ strain), which is designated as region I. After yielding, the fall in G'_M is steeper than the drop in G'_L in both the cases.

This suggests that after yielding, the elastic non-linearity is dominated by strain-rate softening. This is also reflected in the increase in stiffening ratio to about 1 as shown in region II of Fig. 18. While this trend persists for spherical clusters throughout, the decrease in G'_L becomes more pronounced than decrease in G'_M around a strain of 100% for the case of bundles of needles. This implies that the material shifts from a strain-rate softening behavior to strain softening behavior which could possibly be due to complete breakdown of fat network. This is again reflected in the stiffening ratio in region III where the ratio remains around one for spherical clusters, while it decreases for bundles of needles.

Similarly, the corresponding viscous non-linearity measures were further analyzed. Figure 19 is a plot of η'_L (filled) and η'_M (open) as a function of strain amplitude for 25 wt% fat-oil mixtures cooled at 0.1 and 9 K/min. From the onset of non-linear regime till the point of yielding, the decrease

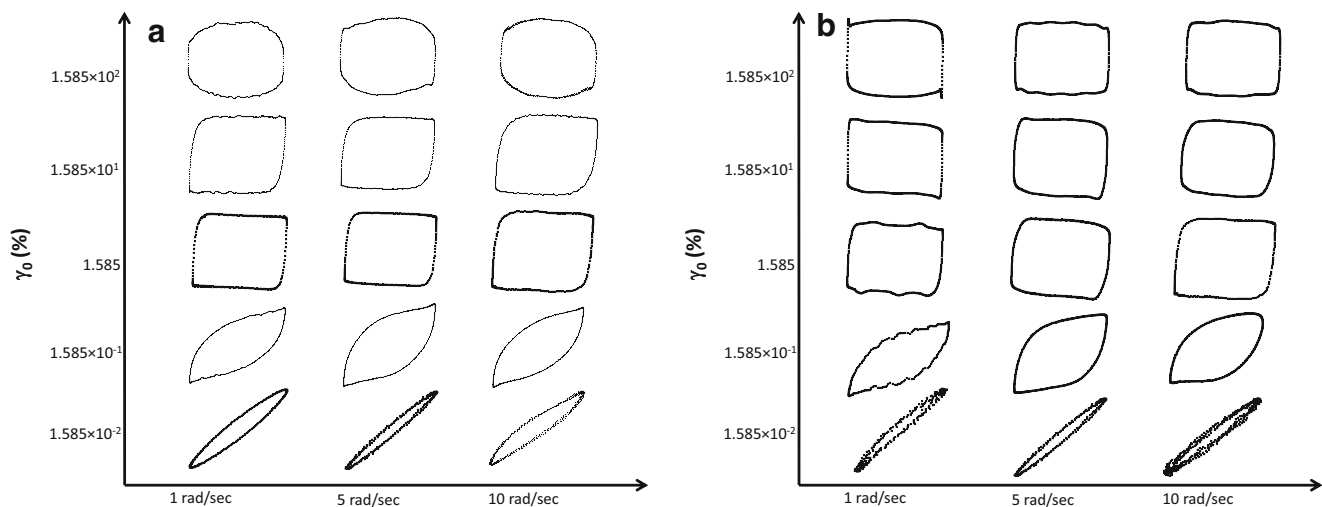


Fig. 15 Pipkin diagrams of of 25 wt% fat-oil mixtures crystallized at 0.1 K/min (**a**) made of bundles of needles and 2 K/min (**b**) made of spherical clusters

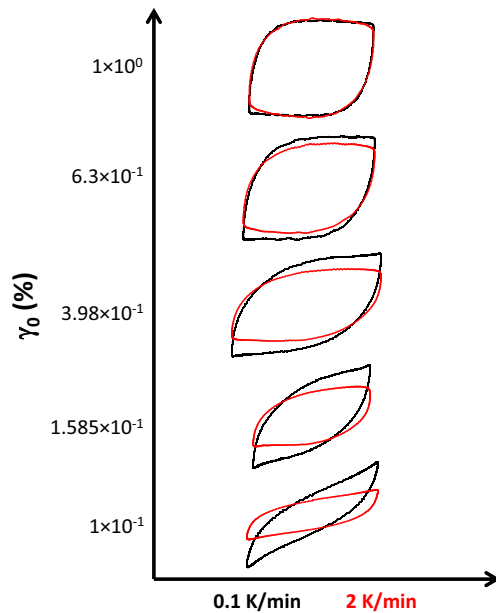


Fig. 16 Evolution of elastic Lissajous-Bowditch plots for different strain amplitude just before and after yielding at a frequency of 10 rad/s for 25 wt% fat-oil at 0.1 and 2 K/min

in η'_M was stronger than η'_L for both types of clusters as seen in region I. This suggests the behavior is predominantly strain thinning. This is also reflected in the thickening ratio (T) in Fig. 20 which increases from $T \sim -0.5$ to $T \sim 0.5$ in region I. After the yield point, both clusters show a decrease in η'_L which is stronger than the decrease in η'_M . This suggests the behavior to be predominantly strain-rate thinning in this region. This is again evident in the thickening ratio which starts to decrease from $T \sim 0.5$ to $T < 0$. The strain-rate thinning is more pronounced in case of bundles

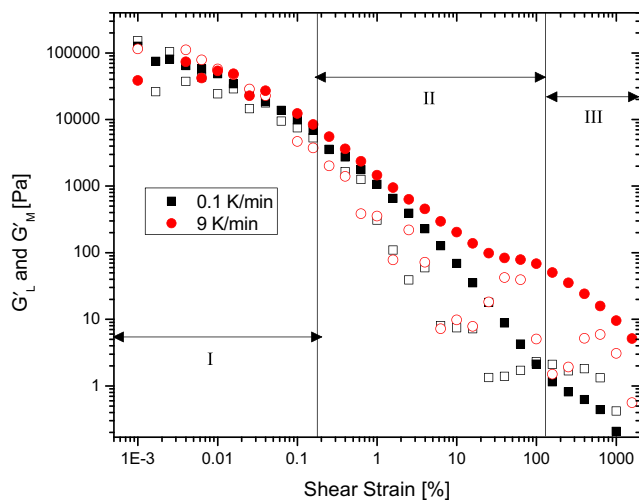


Fig. 17 Elastic non-linear measures G'_L (filled) and G'_M (open) as a function of strain amplitude for 25 wt% fat-oil mixtures cooled at 0.1 and 9 K/min

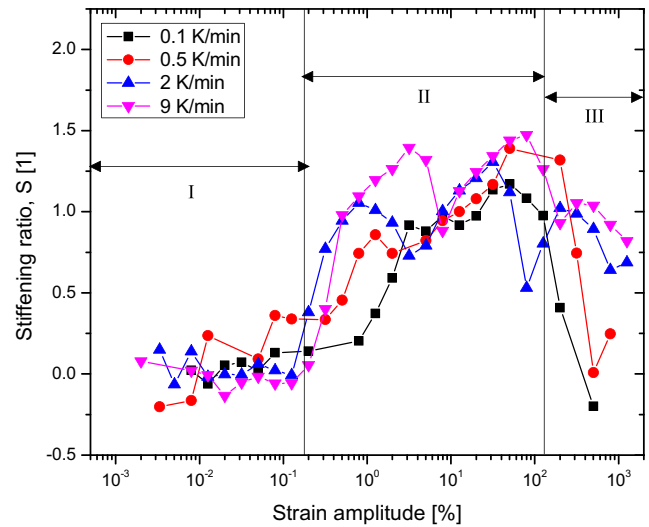


Fig. 18 Stiffening ratio (S) as a function of strain amplitude at 10 rad/s for 25 wt% fat-oil mixtures cooled at 0.1, 0.5, 2, and 9 K/min. Solid line is drawn to guide the eye only

of needles and T value decreases to ~ -1.5 . At a strain of around 100%, the spherical clusters show persistent strain-rate thinning behavior while for bundles of needles, there is again a shift to predominant strain thinning behavior which is reflected in T increasing from $T < 0$ to $T \sim 0$. This again could be due to the complete breakdown of the network made up of bundles of needles while the network made of spherical clusters do not completely breakdown.

To summarize, the following results clearly demonstrate complete breakdown of fat networks made of bundles of needles after yielding:

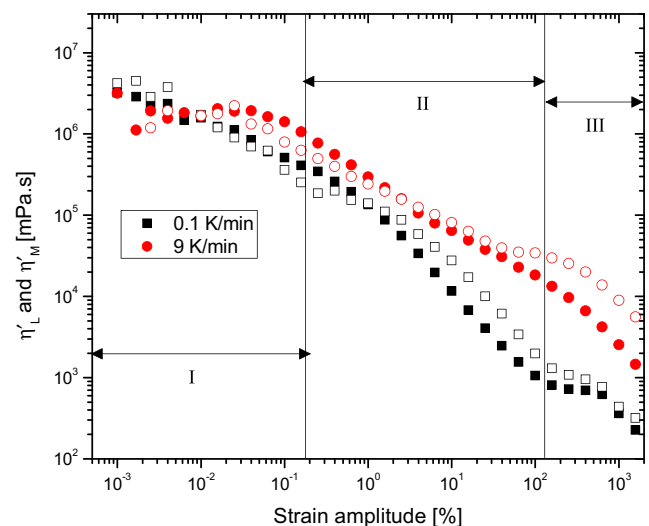


Fig. 19 Viscous non-linear measures η'_L (filled) and η'_M (open) as a function of strain amplitude for 25 wt% fat-oil mixtures cooled at 0.1 and 9 K/min

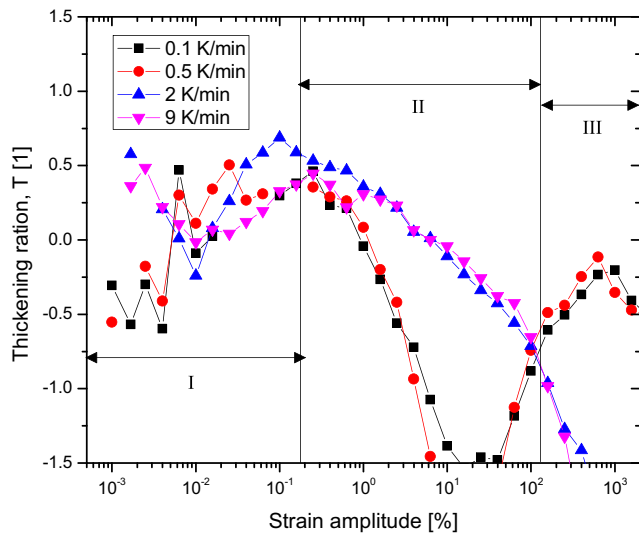
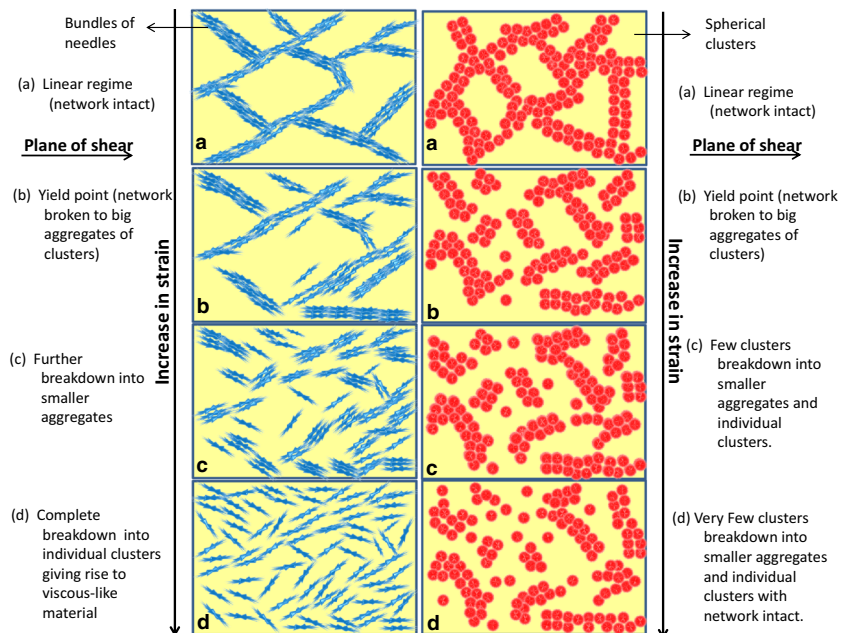


Fig. 20 Thickening ratio (T) as a function of strain amplitude at 10 rad/s for 25 wt% fat-oil mixtures cooled at 0.1, 0.5, 2, and 9 K/min. Solid line is drawn to guide the eye only

1. Decrease in the viscosity values by 2–3 orders of magnitude during the reverse shear rate sweep measurements
2. Steep decrease in G' values and steep increase in strain amplitude values in stress amplitude sweep
3. Viscous signatures after yielding in Lissajous-Bowditch plots of LAOS data
4. Microstructural breakdown as observed from microscopy
5. Non-linear signatures exhibiting predominant strain softening and strain thinning behavior at high strain amplitudes.

Fig. 21 Schematic representation of microstructural evolution of fat crystal networks under shear



Discussion

The results of this study are summarized through a 2D schematic diagram in Fig. 21, which can be used to understand the microstructural evolution of the fat networks comprising clusters of different shapes under shear.

- (a) When the strain amplitude is in the range of 0.001–0.01% (LVR), the clusters remain in an interconnected network encapsulating the oil.
- (b) The onset of non-linear regime is observed at a strain amplitude of 0.01% and beyond a critical strain of about 0.5% (yield point), the continuous interconnected network breaks into large aggregates of clusters and few individual clusters. This initiates the release of encapsulated oil from the fat crystal network.
- (c) With further increase in strain amplitude from 0.5 to 100%, the large aggregates of bundles of needles break down into smaller aggregates and individual clusters. However, in case of spherical clusters, the degree of breakdown is lesser and the most of the bigger aggregates still remain intact. This could possibly be due to the asymmetry of the cluster shape, i.e., the orientation of the clusters will dictate the strength of van der Waals forces and hence may limit further breakdown of clusters.
- (d) At strain amplitudes larger than 100%, the network made of bundles of needles breaks down into individual clusters and becomes a dispersion. In case of spherical clusters, the degree of breakdown is much lesser and the clusters are big enough to form an interconnected network that still holds most of the oil in the pores.

Conclusion

The yielding behavior of fat-oil mixtures made of fat clusters of different shapes, namely, bundles of needles crystallized at low cooling rates (0.1 K/min, 0.5 K/min) and spherical clusters crystallized at high cooling rates (2.0 K/min, 9 K/min), were studied using shear rate sweeps, SAOS, and LAOS measurements. For a given fat concentration, the yield stress values of networks obtained at 0.1 and 0.5 K/min were similar to that of networks obtained at 9 and 2.0 K/min, respectively. However, after yielding, the network made of bundles of needles breaks down to a viscous dispersion while the networks made of spherical clusters did not completely break down and exhibited plastic-like behavior even at high strain amplitudes. This study shows that for a given fat concentration, different cluster shapes can lead to fat networks of similar yield stress values but different behaviors after yielding. Hence, by changing the shape of the constituent cluster in a fat network, desired yield stress and post yield behavior can be engineered for different applications.

Acknowledgements The authors would like to thank Anton Paar (Austria) for providing MCR 702 equipped with twin drive facility. We extend our thanks to Dr. Randy Ewoldt of the University of Illinois, Urbana-Champaign, for sharing the MITlaos software.

References

- Acevedo NC, Marangoni AG (2010) Characterization of the nanoscale in triacylglycerol crystal networks. *Cryst Growth Des* 10(8):3327–3333
- Chen CH, Terentjev EM (2009) Aging and metastability of monoglycerides in hydrophobic solutions. *Langmuir* 25(12):6717–6724. <https://doi.org/10.1021/la9002065>
- da Silva JAL, Coutinho JAP (2004) Dynamic rheological analysis of the gelation behaviour of waxy crude oils. *Rheol Acta* 43(5):433–441
- De Graef V, Depypere F, Minnaert M, Dewettinck K (2011) Chocolate yield stress as measured by oscillatory rheology. *Food Res Int* 44(9):2660–2665
- Ewoldt R, Winter P, McKinley G (2007) Mitlaos version 2.1 beta for matlab. Self-Published, Cambridge
- Ewoldt RH, Hosoi A, McKinley GH (2008) New measures for characterizing nonlinear viscoelasticity in large amplitude oscillatory shear. *J Rheol* (1978-present) 52(6):1427–1458
- Gao P, Zhang J, Ma G (2006) Direct image-based fractal characterization of morphologies and structures of wax crystals in waxy crude oils. *J Phys Condens Matter* 18(50):11,487
- Herrera ML, Hartel RW (2000a) Effect of processing conditions on crystallization kinetics of a milk fat model system. *J Am Oil Chem Soc* 77(11):1177–1188
- Herrera ML, Hartel RW (2000b) Effect of processing conditions on physical properties of a milk fat model system: rheology. *J Am Oil Chem Soc* 77(11):1189–1196
- Khandavalli S, Rothstein JP (2015) Large amplitude oscillatory shear rheology of three different shear-thickening particle dispersions. *Rheol Acta* 54(7):601–618
- Ma L, Barbosa-Cánovas G (1995) Rheological characterization of mayonnaise. Part II: flow and viscoelastic properties at different oil and xanthan gum concentrations. *J Food Eng* 25(3):409–425
- Macias-Rodriguez B, Marangoni AG (2016) Rheological characterization of triglyceride shortenings. *Rheol Acta* 55(9):767–779
- Marangoni AG, Rogers MA (2003) Structural basis for the yield stress in plastic disperse systems. *Appl Phys Lett* 82(19):3239–3241
- Marangoni AG, Acevedo N, Maleky F, Co E, Peyronel F, Mazzanti G, Quinn B, Pink D (2012) Structure and functionality of edible fats. *Soft Matter* 8:1275–1300
- Narine SS, Marangoni AG (1999a) Fractal nature of fat crystal networks. *Phys Rev E* 59:1908–1920
- Narine SS, Marangoni AG (1999b) Relating structure of fat crystal networks to mechanical properties: a review. *Food Res Int* 32(4):227–248
- Narine SS, Marangoni AG (2002) Structure and mechanical properties of fat crystal networks. *Adv Food Nutr Res* 44:33–146
- Ramamirtham S, Shahin A, Basavaraj MG, Deshpande AP (2017) Phase behavior and micro-structure of fat–oil mixtures: engineering the shape of fat clusters. *J Am Oil Chem Soc* 94(1):121–132
- Renou F, Stellbrink J, Petekidis G (2010) Yielding processes in a colloidal glass of soft star-like micelles under large amplitude oscillatory shear (LAOS). *J Rheol* (1978-present) 54(6):1219–1242
- Shih WH, Shih WY, Kim SI, Liu J, Aksay IA (1990) Scaling behavior of the elastic properties of colloidal gels. *Phys Rev A* 42(8):4772
- Suzuki K, Watanabe T (1971) Relationship between assessment and rheological properties of cosmetic creams. *J Texture Stud* 2(4):431–440
- Tang D, Marangoni AG (2006) Microstructure and fractal analysis of fat crystal networks. *J Am Oil Chem Soc* 83(5):377–388
- Toro-Vazquez J, Morales-Rueda J, Dibildox-Alvarado E, Charó-Alonso M, Alonzo-Macias M, González-Chávez M (2007) Thermal and textural properties of organogels developed by candelilla wax in safflower oil. *J Am Oil Chem Soc* 84(11):989–1000
- Vreeker R, Hoekstra L, Den Boer D, Agterof W (1993) The fractal nature of fat crystal networks. *Spec Publ R Soc Chem* 113:16–16